

# Effect of Rare-Earth Additions on the Texture of Wrought Magnesium Alloys: The Role of Grain Boundary Segregation

JOSEPH D. ROBSON

Magnesium alloys that contain certain rare-earth (RE) additions are known to have improved formability and this can be partly attributed to the different texture they display after recrystallization. Previous experimental work has identified segregation of RE to grain boundaries and dislocations as being potentially important in producing this change in behavior. In the present paper, two classical models (Langmuir–McClean and Cahn–Lücke–Stüwe) are used to explore the likely effect of RE additions on grain boundary solute concentration and drag. It is demonstrated that a wide range of RE elements are predicted to segregate strongly to grain boundaries due to the large atomic size misfit with magnesium. The maximum level of segregation is produced for elements such as Y or Gd that combine a high misfit and high bulk solubility. Segregated Y is predicted to produce a solute drag pressure on migrating boundaries several orders of magnitude greater than that obtained by Al or Zn additions. It is demonstrated that while this drag is predicted to be insufficient to strongly retard static recrystallization under typical annealing conditions, it is expected to suppress dynamic recrystallization by any mechanism requiring boundary migration.

DOI: 10.1007/s11661-013-1950-1

© The Minerals, Metals & Materials Society and ASM International 2013

## I. INTRODUCTION

THE benefits that magnesium can offer to transport applications in enabling mass reduction and improving fuel efficiency are hampered by the poor ambient temperature formability of standard wrought magnesium alloys. This means that processes such as cold stamping cannot be directly applied to form magnesium parts. This represents a major barrier to the wider adoption of wrought magnesium alloys. Reducing the critical temperature required to form magnesium alloys is therefore now a topic of intense world-wide research activity (*e.g.*, References 1, 2).

It is clearly understood that part of the cause of the formability problem is the very strong basal textures that tend to be developed in magnesium sheet or extrusions. Reducing the texture strength or changing the texture is therefore one route to improving formability.<sup>[2–4]</sup> This can be achieved by changing the processing route; for example, equal channel angular extrusion, shear rolling, or other novel metal forming methods have been successfully used to alter the texture in magnesium and provide improvements in ductility.<sup>[5,6]</sup> However, alloying is also another attractive route to changing texture. Several alloying additions including Li, Ca, and a range of rare-earth (RE) metals have been shown to be effective in producing a texture change (*e.g.*, References 2, 3, 7–9).

The beneficial effects of RE on the ductility of magnesium alloys was first reported over 60 years ago<sup>[10]</sup> and since then the so called “RE” effect has received considerable attention from the scientific community. The early work on Mg-RE alloys is well documented by Rokhlin.<sup>[11]</sup> In the past decade there has been an intense resurgence of scientific interest in understanding the RE effect in magnesium. The application of new techniques to this problem such as electron backscatter diffraction (EBSD) and atomistic modelling has enabled new insights to be obtained into these materials. Despite these efforts, there is not yet a complete and consistent scientific consensus as to the mechanisms that lead to both texture weakening and improved formability in Mg-RE alloys.

In this paper, a brief overview of the history of developments in understanding the Mg-RE effect is given first. This is not intended to be comprehensive in the manner of a review, but is instead used to highlight some of the key steps in reaching the current understanding of these alloys. The remainder of this paper is devoted to exploring one aspect of the RE effect; the role of grain boundary segregation and solute drag. Simple classical models are used to demonstrate that solute drag is likely to have a critical role in producing the RE effect.

## II. UNDERSTANDING THE RARE-EARTH EFFECT: BACKGROUND

Although a great deal of work was carried out on Mg-RE alloys in the period 1950 to 1990, much of this was focussed on developing high strength, creep resistant cast magnesium alloys. This research led to commercial

---

JOSEPH D. ROBSON, Reader, is with the Physical Metallurgy, Manchester Materials Science Centre, University of Manchester, Grosvenor Street, Manchester M1 7HS, UK. Contact e-mail: joseph.robson@manchester.ac.uk

Manuscript submitted June 18, 2013.

Article published online August 15, 2013

alloys such as WE54 and WE43, which contain a relatively high level of RE addition (approximately 7 to 10 wt pct total) and are precipitation strengthened. These cast alloys were developed into variants that could be extruded, rolled, or forged but the focus was on achieving good elevated temperature strength and corrosion performance rather than texture control. The much weaker texture exhibited in WE alloy when extruded compared to a conventional (non-RE) alloy and its correlation with the greatly reduced mechanical asymmetry was first explicitly noted by Ball and Prangnell.<sup>[12]</sup> The mechanism for texture weakening was not studied, but was speculated to be due to particle stimulated nucleation of recrystallization. However, since many conventional (non-RE) magnesium alloys also contain stable coarse particles but retain a strong basal texture, this mechanism alone would not explain their observations.

Later work revealed that the texture in WE-type extrusions was not random, but contained distinctly different (non-basal) components not observed in non-RE alloys.<sup>[13]</sup> Furthermore, it was shown that the emergence of the unusual texture was associated with recrystallization.<sup>[14]</sup> This is now commonly known as the “RE-texture” following Stanford and Barnett<sup>[2,7,8]</sup> Furthermore, it was demonstrated that the processing conditions (*e.g.*, extrusion temperature) had a critical effect on this texture component; on extruding at a very high temperature, the RE texture was not produced.<sup>[8]</sup>

Work on dilute binary Mg-RE alloys revealed that a texture change could be obtained in Mg-RE alloys even when the level of solute addition was below the solubility limit.<sup>[3,4,8]</sup> The potency of different individual RE elements was also studied. It was shown that the rare-earth effect can be achieved at very low levels of addition, for example only 0.04 at. pct La was needed to achieve a change in texture in an extruded alloy.<sup>[15]</sup> In rolled sheet, as little as 0.03 at. pct Ce was observed to also produce a strong texture weakening effect.<sup>[4]</sup> One remarkable characteristic of the RE effect is that so little addition (*e.g.*, less than 1 in 3000 atoms for Mg-Ce) is needed to produce such a potent change in texture. This observation led to the suggestion that segregation is likely to be important in enabling much higher concentrations than added in the bulk to be achieved locally.<sup>[16,17]</sup>

Once a critical level of RE is achieved, further texture weakening does not occur with more RE addition.<sup>[18]</sup> It was also shown that the potency of an element in weakening the strong basal texture scales inversely with the solubility of the element; *i.e.*, for elements with a higher solubility, more RE is needed to produce a texture change.<sup>[18]</sup> However, this transition was not associated with precipitation, since in all cases the critical RE concentration required to produce the texture weakening effect was below the expected bulk solid solubility.<sup>[15,18]</sup>

The role of shear bands in forming the RE texture component on recrystallization has been noted in several studies, with the RE textured grains in binary Mg-RE extrusions clearly resulting from preferential recrystallization in shear bands.<sup>[8]</sup> More recent work has revealed that the distribution of regions of strain localisation (shear bands or deformation bands) is influenced

directly by RE additions. For example, in studies of a Mg-Y alloy, it has been shown that the addition of yttrium leads to more homogeneously distributed, finer shear bands.<sup>[19]</sup> This has been attributed to the activation of additional non-basal  $\langle c+a \rangle$  slip and a greater propensity for contraction and double twins. This, in turn, is associated with a reduction in the  $I_1$  stacking fault energy (SFE) in the presence of Y.<sup>[19-21]</sup>

Although the effect of RE on the deformation behavior (*e.g.*, shear band formation,  $\langle c+a \rangle$  activity *etc.*) is clearly important in determining the influence of these additions on mechanical properties, it is not alone a sufficient explanation for the texture change seen in RE alloys. This is because as already discussed, the “RE texture” only occurs on recrystallization and unrecrystallized grains typically show textures that are very similar to those in non-RE alloys.<sup>[8,14,17]</sup>

An essential characteristic of RE additions in producing the observed texture change is a potent effect on recrystallization. In particular, RE additions can result in inhibition of dynamic recrystallization (DRX) and a change in DRX mechanism.<sup>[17,22]</sup> Stacking fault energy is clearly important in recovery and recrystallization processes, so the effect of RE additions on SFE is likely to be equally as critical for the recrystallization behavior as it is for the deformation behavior. However, other factors are undoubtedly also important, including the tendency for RE elements to segregate in the microstructure.

Recent experiments have demonstrated that RE elements can segregate strongly to grain boundaries. These data have come from both atom probe<sup>[16]</sup> and energy-dispersive X-ray spectroscopy (EDS) measurements.<sup>[17]</sup> This segregation has been speculated to be responsible for the strong suppression of DRX in Mg-Y alloys.<sup>[17,22]</sup> It was noteworthy that no such segregation was measured for Zn, a conventional alloying addition that does not produce a texture change.<sup>[17]</sup> One factor that is likely to be important in producing the observed segregation of RE elements is the large size misfit between RE and magnesium atoms.

The RE elements all have atomic radii greater than that of magnesium unlike more common alloying elements used in magnesium alloys such as aluminium and zinc. Rokhlin<sup>[11]</sup> has presented a plot of solubility against atomic size mismatch, and an adapted version of this plot is shown in Figure 1. This plot is useful in understanding the different types of behavior seen in RE alloys. The most commonly used RE elements in commercial alloys (or present in RE misch metal<sup>[11]</sup>) are highlighted. It can be seen that the solubility varies over several orders of magnitude and the mismatch in size for the most commonly used RE additions is in the range 10 to 20 pct. As expected, elements with lower misfit have greater solubility. It is also noteworthy that elements in the Y and Ce subgroups lie on two distinct trend lines.

### III. EQUILIBRIUM SEGREGATION

An approximate and widely used equation to predict the tendency for an element to segregate to a grain

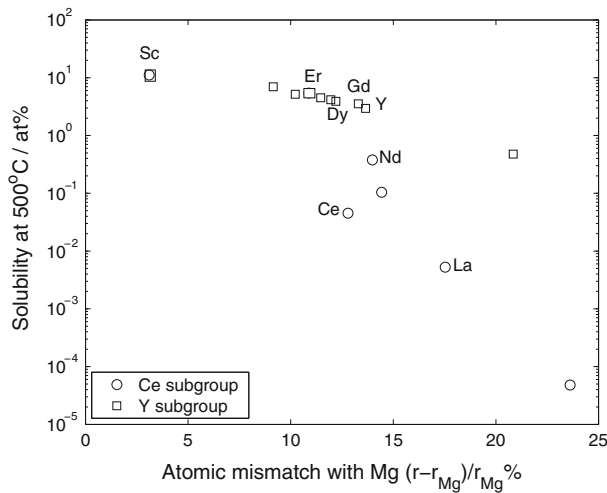


Fig. 1—Solubility plotted against atomic radius mismatch with Mg for various RE additions. Adapted from Rokhlin.<sup>[11]</sup> Note Sc is not usually considered a member of either the Y or Ce subgroups.

boundary (GB) under equilibrium conditions was developed by Langmuir and McLean (LM)<sup>[23]</sup> based on considering the minimum free energy condition for solute atoms to become randomly distributed on GB and grain interior sites given a difference in chemical potential at the two types of site. Assuming the entire GB area is available for segregation, the LM equation gives a relationship between the grain boundary concentration  $X_{GB}$  and bulk concentration  $X_M$  as:

$$\frac{X_{GB}}{1 - X_{GB}} = \frac{X_M}{1 - X_M} \exp\left(\frac{-\Delta G_{seg}}{RT}\right), \quad [1]$$

where  $R$  and  $T$  have their usual meanings and  $\Delta G_{seg}$  is the free energy of segregation (per mole of solute). The contributions to  $\Delta G_{seg}$  include the chemical enthalpy change associated with moving a solute atom from a grain interior to GB site, vibrational, and anharmonic entropy terms, and the elastic strain energy change on moving a misfitting atom to a GB. When the misfit is greater than 10 pct (as is the case for the major RE additions in Mg) the elastic strain energy term is expected to be dominant.<sup>[24]</sup> This term is estimated by assuming all of the elastic strain energy associated with the misfitting solute embedded in the matrix is relieved when the solute atom segregates to the grain boundary and is given (per atom) by:<sup>[24]</sup>

$$E_{el} = \frac{24\pi K G r^3 \xi^2}{3K + 4G} \quad [2]$$

where  $K$  is the solute bulk modulus,  $G$  is the solvent (matrix) shear modulus,  $r$  is the radius of the solute atom in the lattice, and  $\xi = (r_1 - r_0)/r_1$  where  $r_1$  is the radius of the solute atom (unstrained) and  $r_0$  is the radius of the site in which the solute sits. The radius of the solute atom in the matrix and the radius of the site in which the atom sits in the matrix are often taken to be equal to the radius of the solvent atom, *i.e.*, in the present work  $r = r_0 = r_{Mg}$  where  $r_{Mg}$  is the atomic

radius of magnesium. Although the LM approach ignores many of the complexities associated with GB segregation it is qualitatively useful in allowing comparisons to be made between the expected behavior of different RE elements. All the input data required by the model were taken from Rokhlin.<sup>[11]</sup>

Figure 2(a) shows the calculated value of  $\Delta G_{seg}$  for seven RE elements covering a range of misfit sizes and solubilities. As expected from the simple LM approach, the largest interaction energy is associated with elements that have the greatest misfit with magnesium (*e.g.*, La). Also shown is an estimate of  $\Delta G_{seg}$  for the Mg-Y system derived by Hadorn *et al.*<sup>[17]</sup> from experimental measurements of segregation in this system. It can be seen that the purely elastic approach of LM underestimates  $\Delta G_{seg}$  by a factor of approximately two, implying that the chemical contribution to the free energy of segregation may be significant. However, in allowing a comparison to be made between of the tendency for segregation of different RE elements, the simple LM method is adequate.

Once  $\Delta G_{seg}$  is known, the grain boundary concentration of RE can be estimated. This calculation was first performed for a fixed composition of 0.22 at. pct and a temperature of 673 K (400 °C), chosen to match the conditions used by Hadorn *et al.* in their experimental study of Mg-Y.<sup>[17]</sup> Figure 2(b) shows the predicted grain boundary concentrations for these conditions. Also shown is the experimental measurement for the Mg-Y system; the model underpredicts the tendency for segregation by about a factor of 2. Stanford *et al.*<sup>[16]</sup> have published data on grain boundary segregation in a Mg-Gd extrusion. A direct comparison with this study is difficult since the solute level on the boundaries was determined in the as-deformed conditions and is likely to deviate from equilibrium. Nevertheless, a similar discrepancy was observed between the model predictions for this alloy and the measurements. For example, after extrusion at 783 K (510 °C) a Mg—0.23 at. pct Gd alloy showed a measured level of RE on the GBs of approximately 1.1 at. pct,<sup>[16]</sup> which is about twice that predicted by the model for the same bulk concentration and temperature. It is thus reasonable to suppose that these predictions represent an underestimate of the true tendency for RE elements to segregate by about a factor of 2.

Figure 2(b) suggests that elements such as La and Ce should produce the highest GB concentrations. This will be true for a given level of RE addition, but only if the solubility limit is not exceeded. The limit imposed by solubility was ignored in producing Figure 2(b) and for the low solubility elements (La, Ce) the assumed bulk concentration is above the solubility limit.

When the amount of alloying element in bulk is assumed to be at the maximum solubility limit [at 773 K (500 °C)] a different picture emerges, as shown in Figure 2(c). Elements such as La and Ce have such low solubility that even though they are predicted to segregate strongly, they are expected to produce the lowest concentration of RE on the grain boundaries. Any La or Ce added in excess of the solubility limit will be in the form of precipitates and will not be free to

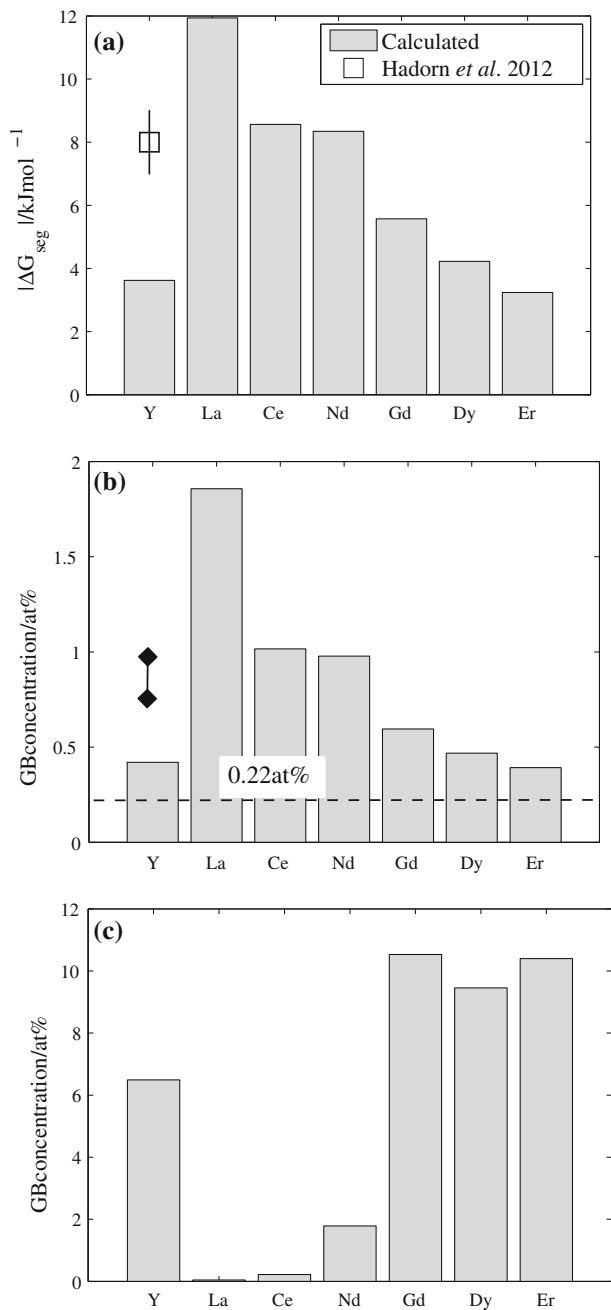


Fig. 2—Predictions from Langmuir–McLean model for grain boundary segregation for a range of RE additions (a) free energy of segregation per mole solute (b) grain boundary concentration at 673 K (400 °C), assuming a mean RE concentration of 0.22 at. pct. (c) grain boundary concentration at 673 K (400 °C), assuming a mean RE concentration at the solubility limit. Experimental data for Mg-Y from Ref. [17].

segregate to the boundaries. For such elements, the Zener drag effect<sup>[25]</sup> due to these precipitates is likely to be more important than the solute drag effect.

Considering the solute effect only, Figure 2(c) suggests that RE elements in the yttrium subgroup Y and Gd have the potential to produce the highest RE concentration on GBs since they combine a strong tendency to segregate with a relatively high solubility.

Application of the LM model to Al and Zn is problematic since for both elements the misfit is below the level where the relaxation of elastic strain energy is expected to be the dominant effect controlling  $\Delta G_{\text{seg}}$ . Ignoring this difficulty gave a tendency for segregation for both elements that was always less than 15 pct in excess of the bulk concentration (*i.e.*, no strong tendency to segregate). This is consistent with the limited observations available in the Reference 17.

#### IV. SOLUTE DRAG

It has been demonstrated above that RE elements are predicted to segregate strongly to grain boundaries at equilibrium. They might therefore be expected to have a significant effect on the mobility of such boundaries. However, the effect of any solute on boundary mobility also depends on the diffusivity of that species within both the bulk and the boundary itself. It is the combination of the free energy difference driving segregation and diffusion behavior that ultimately determine the drag that a solute will impose on the grain boundary. The classical treatment for this problem is the Cahn–Lücke–Stüwe (CLS) impurity drag model.<sup>[26,27]</sup>

In the present work, this model was applied to predict the drag effect expected due to yttrium (RE) compared to Al and Zn, the two most common non-RE additions used in magnesium alloys. Unfortunately, a lack of diffusion data for the other RE elements in magnesium meant it was not possible to extend the analysis to compare different RE elements. Even for yttrium, there is no experimental data on the grain boundary diffusivity, and so an estimate has to be made. Due to this and the other approximations inherent in the model, the predictions are not expected to be quantitatively accurate. However, they do enable a sensible qualitative comparison to be made between solutes.

In the CLS model, the grain boundary is characterized as being a site with a local change in free energy and diffusivity of solute atoms compared to that in the matrix. Various assumptions can be used to determine the width over which these special conditions apply and represent the transition from GB to grain interior conditions and a priori it is difficult to know which is correct.<sup>[28]</sup> Therefore, in this work, the simple assumption was used that there is a linear transition in both  $D$  and  $\Delta G$  over a distance  $\delta$  from the grain boundary. This is shown schematically in Figure 3.

According to the CLS model the drag pressure due to solute is given by:<sup>[26]</sup>

$$P_d = \frac{\alpha v X_M}{1 + \beta^2 v^2} \quad [3]$$

where  $v$  is the boundary velocity and  $\alpha$  and  $\beta$  are parameters that for the diffusion and free energy profiles assumed here (Figure 3) are obtained from:<sup>[28]</sup>

$$a = \frac{RT}{\delta G_{\text{seg}}} \log \left( \frac{D}{D_{\text{GB}}} \right) \quad [4]$$



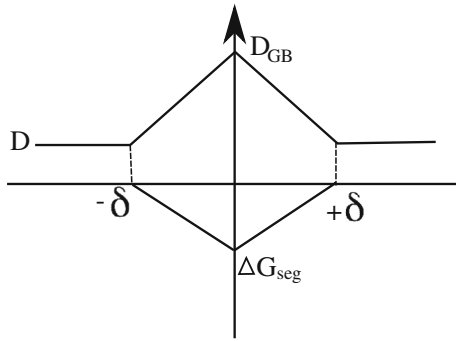


Fig. 3—Sketch showing the assumed variation of diffusion coefficient and free energy of segregation in the vicinity of a grain boundary located at  $x = 0$ .

$$\alpha = \frac{4R^2T^2}{V_m G_{seg}^2 D a^3 - a} \quad [5]$$

$$\frac{\alpha}{\beta^2} = \frac{2G_{seg}D_{GB}}{V_m a} \left(1 - \frac{D}{D_{GB}}\right) \quad [6]$$

where  $D$  is the bulk diffusion coefficient of solute,  $D_{GB}$  is the grain boundary diffusion coefficient, and  $V_m$  the molar volume. For yttrium in Mg,  $D_0$  and  $Q$  for bulk diffusion were given by Stloukal *et al.* in Reference 29, for zinc in Mg by Čermák *et al.* in Reference 30, and for Al in Mg by Moreau *et al.* in Reference 31. Since the appropriate values for GB diffusion are not known, the commonly used approximation was made that  $Q_{GB} \approx 0.5Q$ .<sup>[32]</sup>

The CLS model provides a relationship between the boundary velocity and drag pressure. Figure 4 shows this relationship predicted for yttrium, aluminium, and zinc in magnesium at 723 K (450 °C) with a solute content of 1 at. pct in each case. A 1 at. pct solute concentration corresponds to a wt pct concentration of 3.5, 1.1, and 2.6 for Y, Al, and Zn respectively. This solute concentration is used as a standard in all further calculations unless otherwise stated. Note that the sensitivity of the drag pressure to mean solute concentration is much less than the order of magnitude effects of temperature or boundary velocity.

The CLS model predicts there are two distinct regimes, one where the drag pressure increases as boundary velocity increases and one where the drag pressure decreases with increasing boundary velocity. The maximum drag effect occurs at the transition between the regimes. The physical interpretation of this transition is the change from a low velocity regime where an enriched solute region can be dragged along with the boundary to a high velocity regime where the boundary breaks away from the solute enriched region. Cahn demonstrated that in the low velocity limit, slower diffusing solutes will lead to greater drag, whereas in the high velocity limit the opposite is true.<sup>[26]</sup>

For the reasons already discussed, the approximations necessary in the present work means that the quantitative

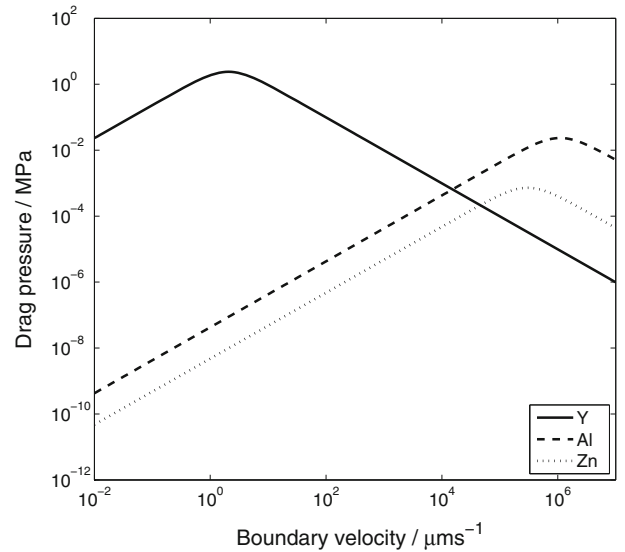


Fig. 4—Predicted solute drag pressure as a function of boundary velocity at 723 K (450 °C) for 1 at. pct addition of Y, Al, and Zn to Mg.

predictions are not expected to be accurate. However, for a qualitative comparison between the effects of Y, Al, and Zn, the results are valid and reveal interesting behavior (Figure 4). First, it can be seen that the drag pressure exerted by Y is predicted to be much greater (by several orders of magnitude) than that of Al or Zn unless the boundary velocity is much higher than would be expected during conventional processing (on the order of  $1 \text{ cm s}^{-1}$ ). Second, for Al and Zn the drag pressure falls within the low velocity regime across the whole range of likely boundary velocities. For Y, the transition between regimes (and thus the maximum drag pressure) occurs at a boundary velocity of approximately  $1 \text{ } \mu\text{m s}^{-1}$ , which is much closer to the boundary velocities expected in practice (as discussed below).

A very approximate estimate of typical boundary velocity during recrystallization of Mg-RE alloys can be obtained from static recrystallization experiments. For example, Stanford reports results from static recrystallization of a Mg—1.3 wt pct Gd alloy at 723 K (450 °C) after deformation at 673 K (400 °C) and a strain rate of  $10 \text{ s}^{-1}$ , a condition which produced  $<15 \text{ pct DRX}$ .<sup>[33]</sup> This alloy was fully recrystallized after 1 h annealing with a maximum grain size of  $\approx 70 \text{ } \mu\text{m}$ . Ignoring the effects of impingement, and assuming the largest grains recrystallized grains nucleated at the start of annealing and grew isotropically this gives an average boundary velocity of  $\approx 10 \text{ nm s}^{-1}$ . Clearly, this value will be sensitive to temperature, stored energy *etc.*, but it is a reasonable order of magnitude estimate of the boundary velocity during recrystallization of magnesium alloys under typical conditions.

Calculations of the drag effect were performed using this value of boundary velocity but with a variation in temperature. The predictions are shown in Figure 5. Across the whole temperature range, the predicted drag due to Y is several orders of magnitude greater than that due to Al or Zn. The peak in the drag due to Y is also at

a higher temperature than that due to Al or Zn. A result of this is that the temperature ranges used for practical hot working and recrystallization treatments in magnesium are much closer to the temperature that leads to maximum drag for Y than for Al or Zn solutes.

Although the model is not expected to be quantitatively accurate, it is useful to make some crude comparisons of the predicted drag pressure with the driving pressures expected for recrystallization and grain growth. For example, for recrystallization of a deformed structure, a driving pressure in the range 2 to 20 MPa is typical, whereas for grain growth a driving pressure in the range 0.01 to 1 MPa is expected.<sup>[25]</sup>

To compare the driving and drag pressures for boundary motion it is necessary to also include the intrinsic drag pressure as well as the solute drag effect. The intrinsic drag coefficient is the reciprocal of the boundary mobility in the absence of solute. Following Cahn, it is assumed that the intrinsic drag pressure ( $P_i$ ) scales linearly with boundary velocity, giving:<sup>[26,34]</sup>

$$\lambda = \frac{V_m}{2D_{GB}^{Mg}\delta RT} \quad [7]$$

$$P_i = \lambda v, \quad [8]$$

where  $D_{GB}^{Mg}$  is the grain boundary self diffusion coefficient of magnesium for which the activation energy and pre-factor are given by Crossland and Jones.<sup>[35]</sup> Figure 6 shows both the solute, intrinsic, and total drag pressures for the case of yttrium solute and a boundary velocity of  $10 \text{ nm s}^{-1}$ . It can be seen that for all temperatures  $>423 \text{ K}$  ( $150 \text{ }^\circ\text{C}$ ), the predicted drag pressure in the presence of Y is almost entirely due to solute drag.

The total drag effect (intrinsic + solute drag) can now be compared with the expected driving pressure for recrystallization and grain growth as a function of

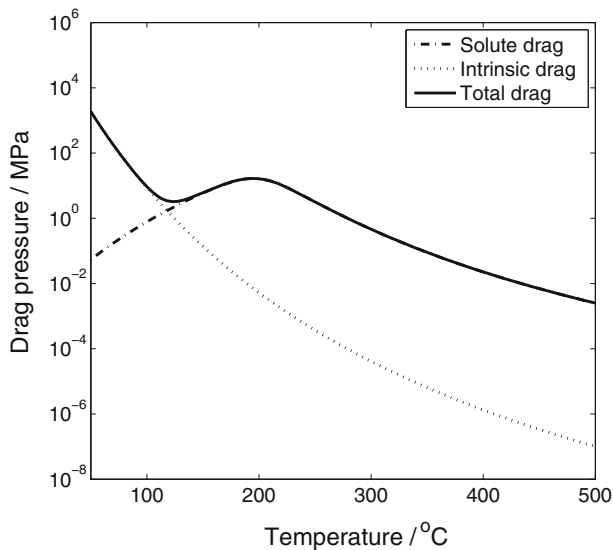


Fig. 5—Predicted solute drag pressure as a function of temperature for a boundary velocity of  $10 \text{ nm s}^{-1}$  for 1 at. pct addition of Y, Al, and Zn to Mg.

temperature and boundary velocity as shown in Figure 7 (contour map). Regions where the drag pressure exceeds the expected driving pressure are shown for both static recrystallization and grain growth. Also marked for reference is the boundary velocity of  $10 \text{ nm s}^{-1}$  that has been taken as a typical value during recrystallization. Note that this map is not expected to be quantitatively accurate, but does demonstrate some interesting features.

The first of these is that Y solute is predicted to produce a drag effect that is insufficient to prevent static recrystallization during annealing since the drag pressure is an order of magnitude less than the driving pressure expected for recrystallization at any temperature above  $523 \text{ K}$  ( $250 \text{ }^\circ\text{C}$ ). Even when the calculation was repeated with a bulk Y concentration at its

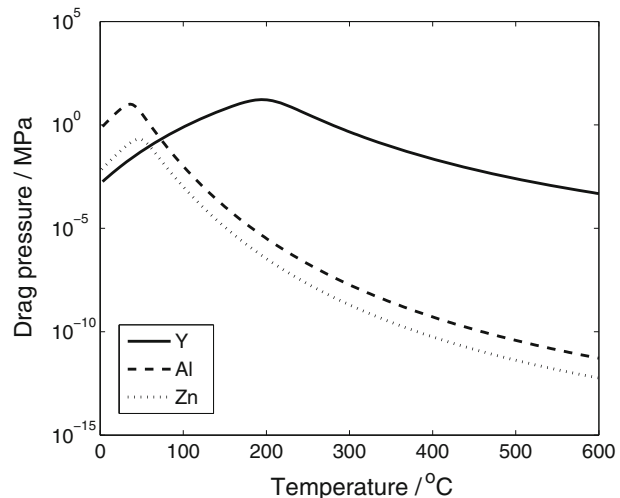


Fig. 6—Predicted solute drag, intrinsic drag, and total drag pressure as a function of temperature for a boundary velocity of  $10 \text{ nm s}^{-1}$  for Mg—1 at. pct Y.

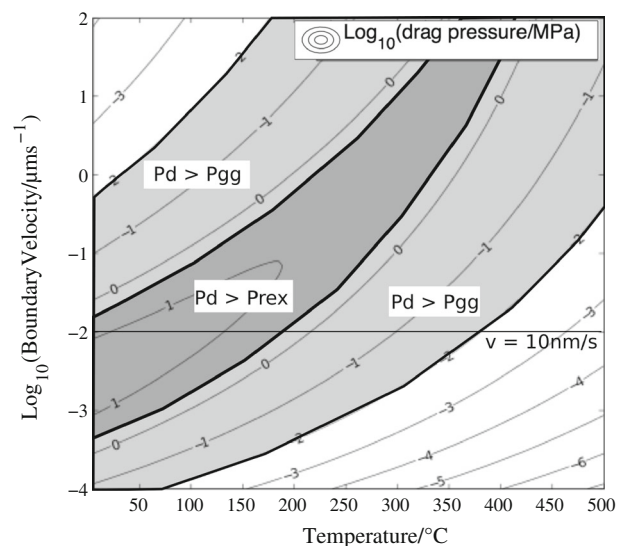


Fig. 7—Contour map showing the logarithm of the predicted total drag pressure for Mg—1 at. pct Y as a function of temperature and boundary velocity. Marked on the map are regions where the drag pressure is expected to exceed the driving pressure for grain growth and recrystallization.

maximum solubility in magnesium (12 wt pct, 3.6 at. pct),<sup>[11]</sup> the total drag pressure predicted remained less than half the expected driving pressure for recrystallization at any temperature >523 K (250 °C). Furthermore, this drag pressure decreases rapidly with an increase in temperature. Therefore, even at its maximum possible concentration in solution, Y is not expected to strongly inhibit static recrystallization by solute drag.

Second, as expected, grain growth is predicted to be suppressed over a much wider of conditions and thus it is likely that as the driving force for grain growth dissipates, there will reach a point where Y solute effectively stalls the process. Finally, it can be seen that as the boundary velocity is increased, the window in which the most potent pinning effect is predicted moves to higher temperature, closer to the typical temperatures used for hot working of magnesium. This is likely to have important consequences for the effect of Y solute on DRX, discussed next.

It has been observed that RE elements such as Y can strongly suppress DRX in magnesium.<sup>[17,22]</sup> DRX is complex and can occur by a number of different mechanisms.<sup>[36]</sup> However, many of mechanisms such as strain-induced boundary migration (SIBM) require the movement of grain boundaries. This movement must occur more rapidly than that assumed for static recrystallization since the time available for DRX is usually on the order of seconds (or less). This requires boundary velocities in the range 1 to 10  $\mu\text{m s}^{-1}$  to produce typical DRX grain sizes observed after hot deformation. For these velocities, Figure 7 demonstrates that the peak drag effect is predicted in the range 523 K to 623 K (250 °C to 350 °C), and is sufficiently large to exceed the driving force for recrystallization. This implies that one reason that DRX is so strongly suppressed by Y additions is that typical processing temperatures coincide with the conditions that produce the peak drag effect, suppressing DRX by boundary migration. Note that this is not the case for Al and Zn solutes, where the peak drag effect is predicted at much lower temperature (below the practical recrystallization temperature), even for the higher boundary velocities required for DRX.

In summary, the CLS model suggests that Y is more potent than Al and Zn in producing drag on migrating boundaries for three reasons. First, the driving force for Y to segregate to grain boundaries is greater than that for Al and Zn due to the large size mismatch. Second, the diffusion rate of Y in magnesium is lower than that of Al or Zn. Finally, the peak in the drag pressure expected for Y occurs at a temperature and boundary velocity that are much closer to those expected in practical hot processing and annealing of magnesium alloys. In particular, for boundary velocities expected for DRX, the peak drag effect occurs at a temperature that falls within the range typically used for hot working of magnesium.

Although this analysis has only been performed for one RE element (Y) other RE elements also have a strong tendency to segregate to boundaries and are expected to diffuse slowly in magnesium. Therefore, it is reasonable to expect that similar behavior might be

expected for other RE additions. In particular other yttrium subgroup additions such as Gd that are similar in solubility and misfit might be expected to behave in a very similar way.

Solubility is also an important factor on the ability of a solute to produce a drag effect on a boundary. The solute drag effect increases with higher levels of alloying elements in solution. However, in alloys where the solubility limit is exceeded, precipitation can occur along grain boundaries. This will also have a potent effect in retarding grain boundary migration.<sup>[37]</sup> This effect with be particularly important for RE elements that have low solubility at typical processing temperatures.

Segregation of solute to dislocations is undoubtedly also important in producing some of the effects attributed to RE elements. Although this has not been considered in the present paper, it is noted that the classical theory for segregation to dislocations has many features in common with the CLS model for solute drag. For example, in classical theory, segregation to dislocations is driven mainly by the local relaxation of the misfit strain that can occur in the strain field around a dislocation.<sup>[38]</sup> Therefore, for the same reasons discussed here, a strong tendency for RE to segregate to dislocations and inhibit their motion would be expected.

As Stanford<sup>[33]</sup> has discussed, a strong suppression of dynamic restoration processes by RE can lead to a much greater stored energy in the as-deformed state compared to non-RE alloys. This can lead to faster SRX in a RE containing alloy<sup>[33]</sup> but this can occur even if the boundary drag is increased by RE additions. This is because the overall kinetics are a competition between driving and drag pressures, both of which are influenced by RE additions. The experimental evidence suggests that RE is most effective in suppressing the dynamic restoration processes (DRX and dynamic recovery) that occur during deformation, thus enabling a higher stored energy to be retained prior to annealing and SRX.<sup>[33]</sup> This supposition is supported by the model predictions presented here.

Finally, at high temperatures [*e.g.*, 773 K (500 °C)], the solute drag model predicts that under all conditions the drag pressure is small (<0.1 MPa). This is a plausible explanation for the disappearance of the RE texture when deformation occurs at such high temperatures.<sup>[8]</sup> In this regime, the predicted drag pressure is unlikely to be sufficient to suppress DRX sufficiently to enable the deformation heterogeneities to persist in the microstructure that appear to generate the RE texture on recrystallization.

## V. CONCLUSIONS

In this paper, classical models for solute segregation to grain boundaries and solute drag have been used to investigate the hypothesis that these effects are critical to produce the observed change in recrystallization behavior and texture evolution widely noted in magnesium alloys containing RE additions. The following conclusions can be drawn from this work.

1. The LM model for equilibrium segregation to grain boundaries predicts that RE elements will segregate strongly to boundaries, producing a concentration on the boundary that is at least twice that in the bulk at 673 K (400 °C). This is due to the large size mismatch between RE and Mg atoms. Zn and Al are not predicted to segregate strongly to boundaries.
2. The predicted maximum possible concentration of RE solute on boundaries at equilibrium occurs for high solubility additions such as Y, Gd, Dy, and Er (all in the Y-subgroup) since these elements have both a large misfit and relatively high solubility in bulk magnesium.
3. The CLS model for solute drag has been used to compare the predicted drag effect of Y with Al and Zn on grain boundary motion. It has been demonstrated that for practical temperatures and boundary velocities, Y is predicted to produce a drag pressure several orders of magnitude greater than Al or Zn. This is due to both the high tendency of Y to segregate to boundaries, and the low diffusivity of Y in Mg.
4. The CLS model predicts that Y will not produce a maximum solute drag effect sufficient to strongly suppress static recrystallization for typical static annealing temperatures and expected boundary velocities
5. The CLS model predicts that Y but not Al or Zn will have a strong retarding effect on DRX by boundary migration. This is because the conditions (temperature and boundary velocity) that produce the maximum solute drag effect due to Y are coincident with the conditions for DRX in magnesium.

## REFERENCES

1. S.R. Agnew: *JOM*, 2004, vol. 56, pp. 20–21.
2. M.R. Barnett, N. Stanford, P. Cizek, A. Beer, Z. Xuebin, and Z. Keshavarz: *JOM*, 2009, vol. 61, pp. 19–24.
3. J. Bohlen, M.R. Nürnberg, J.W. Senn, D. Letzig, and S.R. Agnew: *Acta Mater.*, 2007, vol. 55, pp. 2101–22.
4. K. Hantzsche, J. Wendt, K.U. Kainer, J. Bohlen, and D. Letzig: *JOM*, 2009, vol. 61, pp. 38–42.
5. S.R. Agnew, M.H. Yoo, and C.N. Tomé: *Acta Mater.*, 2005, vol. 53, pp. 3135–46.
6. S. Kim, B. You, C.D. Yim, and Y. Seo: *Mater. Lett.*, 2005, vol. 59, pp. 3876–80.
7. N. Stanford, D. Atwell, A. Beer, C. Davies, and M.R. Barnett: *Scripta Mater.*, 2008, vol. 59, pp. 772–75.
8. N. Stanford and M.R. Barnett: *Mater. Sci. Eng. A*, 2008, vol. 496, pp. 399–408.
9. L.W.F. Mackenzie and M.O. Pekguleryuz: *Scripta Mater.*, 2008, vol. 59, pp. 665–68.
10. T.E. Leontis: *J. Met.*, 1951, vol. 3, pp. 987–93.
11. L.L. Rokhlin: *Magnesium Alloys Containing Rare Earth Metals*, Taylor and Francis, London, 2003.
12. E.A. Ball and P.B. Prangnell: *Scripta Metall. Mater.*, 1994, vol. 31, p. 111.
13. L.W.F. Mackenzie, B. Davis, F.J. Humphreys, and G.W. Lorimer: *Mater. Sci. Technol.*, 2007, vol. 23, pp. 1173–80.
14. J.W. Senn and S.R. Agnew: *Magnesium Technology*, TMS, Warrendale, PA, 2008.
15. N. Stanford: *Mater. Sci. Eng. A*, 2010, vol. 527, pp. 2669–77.
16. N. Stanford, G. Sha, J. Xia, S.P. Ringer, and M.R. Barnett: *Scripta Mater.*, 2011, vol. 65, pp. 919–21.
17. J.P. Hadorn, K. Hantzsche, S.B. Yi, J. Bohlen, D. Letzig, J.A. Wollmershauser, and S.R. Agnew: *Metall. Mater. Trans. A*, 2012, vol. 43A, pp. 1347–62.
18. K. Hantzsche, J. Bohlen, J. Wendt, K. Kainer, S. Yi, and D. Letzig: *Scripta Mater.*, 2010, vol. 63, pp. 725–30.
19. S. Sandlöbes, S. Zaeferrer, I. Schestakow, S. Yi, and R. Gonzalez-Martinez: *Acta Mater.*, 2011, vol. 59, pp. 429–39.
20. S. Sandlöbes, M. Friák, J. Neugebauer, and D. Raabe: *Mater. Sci. Eng. A*, 2013, vol. 578, pp. 61–68.
21. Q. Zhang, L. Fu, T. Fan, B. Tang, L. Peng, and W. Ding: *Phys. B*, 2013, vol. 416, pp. 39–44.
22. R. Cottam, J.D. Robson, G. Lorimer, and B. Davis: *Mater. Sci. Eng. A*, 2008, vol. 485, pp. 375–82.
23. D. McLean: *Grain Boundaries in Metals*, Oxford University Press, Oxford, 1957.
24. M.P. Seah: *J. Phys. F*, 1980, vol. 10, pp. 1043–46.
25. F.J. Humphreys and M. Hatherly: *Recrystallization and Related Annealing Phenomena*, Pergamon, Oxford, 1996.
26. J.W. Cahn: *Acta Metall.*, 1962, vol. 10, pp. 789–98.
27. Lücke K., Stüwe H.P: in *Recovery and Recrystallization of Metals*, L. Himmell, ed., Interscience, New York, NY, 1963, pp. 171–76.
28. P. Gordon and R.A. Vandermeer: *Recrystallization, Grain Growth, and Textures*, ASM, Materials Park, OH, 1965.
29. I. Stloukal and J. Čermák: *J. Alloys Compd.*, 2009, vol. 471, pp. 83–89.
30. J. Čermák and I. Stloukal: *Compos. Sci. Technol.*, 2008, vol. 68, pp. 417–23.
31. G. Moreau, J.A. Cornet, and D. Calais: *J. Nucl. Mater.*, 1971, vol. 25, pp. 197–202.
32. J.W. Christian: *Theory of Transformations in Metals and Alloys*, Pergamon, Oxford, 1975.
33. N. Stanford: *Mater. Sci. Eng. A*, 2013, vol. 565, pp. 469–75.
34. G.T. Higgins: *Met. Sci.*, 1974, vol. 8, pp. 143–50.
35. I.G. Crossland and R.P. Jones: *Met. Sci.*, 1977, vol. 11, pp. 504–08.
36. A. Galiyev, R. Kaibyshev, and G. Gottstein: *Acta Mater.*, 2011, vol. 49, p. 1199.
37. J.P. Hadorn, K. Hantzsche, S.B. Yi, J. Bohlen, D. Letzig, and S.R. Agnew: *Metall. Mater. Trans. A*, 2012, vol. 43A, pp. 1363–75.
38. J.W. Cahn: *Acta Metall.*, 1957, vol. 5, pp. 169–72.